MgO/h-BN 复合载体对 Ba-Ru/MgO/h-BN 氨合成催化剂性能的影响

杨晓龙[1,2]，唐立平[1,2]，夏春谷[1]，熊绪茂[1]，慕新元[1]，胡　斌[1,*]

[1]中国科学院兰州化学物理研究所羰基合成与选择氧化国家重点实验室, 甘肃兰州 730000

[2]中国科学院研究生院, 北京 100049

摘要: 采用浸渍法制备了系列不同质量比的 MgO/h-BN 复合载体负载的 Ru 基氨合成催化剂, 采用 X 射线衍射、N$_2$ 低温物理吸附、X 射线荧光、扫描电镜、透射电镜、程序升温分析等手段对催化剂进行了详细的表征, 并在固定床反应器上考察了它们在氨合成反应中的催化性能. 结果表明, MgO/h-BN 复合载体中 h-BN 含量对催化剂活性的影响较大, Ba-Ru[1:1] (摩尔比)/MgO/h-BN[8:2] (质量比), Ba-Ru[1:1]/MgO/h-BN[6:4]和 Ba-Ru[1:1]/MgO/*h*-BN[5:5]催化剂上氨合成活性均高于 Ba-Ru/MgO 催化剂. 在 425 °C, 5.0 MPa, N$_2$/H$_2$ = 1/3 和 5000 h^{-1} 条件下, Ba-Ru[1:1]/MgO/*h*-BN[8:2]表现出最优催化活性, 达 506.9 ml/(g$_{cat}$·h). 这可归因于 MgO/h-BN 复合载体上存在较高数量的碱性位, 特别是弱碱性位和中等强度碱性位, 而这些碱性位可能是由 MgO 和 h-BN 之间的相互作用造成.

关键词: 氨合成; 钌催化剂; 氧化镁; 六方氮化硼; 碱性

中图分类号: O643/TQ113.2 　　　**文献标识码**: A

Effect of MgO/h-BN Composite Support on Catalytic Activity of Ba-Ru/MgO/h-BN for Ammonia Synthesis

YANG Xiaolong[1,2], TANG Liping[1,2], XIA Chungu[1], XIONG Xumao[1], MU Xinyuan[1], HU Bin[1,*]

[1]*State Key Laboratory for Oxo Synthesis and Selective Oxidation, Lanzhou Institute of Chemical Physics, Chinese Academy of Sciences, Lanzhou 730000, Gansu, China*

[2]*Graduate University of Chinese Academy of Sciences, Beijing 100049, China*

Abstract: A series of MgO/hexagonal boron nitride (h-BN) composite with different mass ratio were synthesized by impregnation method and used as supports for ruthenium catalysts in ammonia synthesis reaction. The catalysts were characterized by X-ray diffraction, N$_2$ physical adsorption, X-ray fluorescent spectrometer, scanning electron microscope, transmission electron microscope, temperature programmed reduction of H$_2$, and temperature programmed desorption of CO$_2$ (CO$_2$-TPD). The activity measurements of ammonia synthesis were carried out in a fixed-bed flow reactor with a mixture of N$_2$ and H$_2$ atmosphere under steady-state conditions (5.0 MPa, 350–500 °C, 5000 h^{-1}). The results showed that the rate of ammonia formation was strongly influenced by the h-BN content used in the catalysts preparation process. The Ba-Ru[1:1] (molar ratio of Ba to Ru = 1:1)/MgO/h-BN[8:2] (weight ratio of MgO to h-BN = 8:2), Ba-Ru[1:1]/MgO/h-BN[6:4] and Ba-Ru[1:1]/MgO/h-BN[5:5] catalysts exhibited higher activity than Ba-promoted Ru/MgO catalyst. At 425 °C, 5.0 MPa, flow rate of 5000 h^{-1}, and a N$_2$/H$_2$ = 1/3 atmosphere, the optimum activity of 506.9 ml/(g$_{cat}$·h) was achieved when MgO/h-BN[8:2] was used as the catalytic support. The execllent activity was mainly attributed to the basicity of the MgO/h-BN combination-type support, especially "weak" and "medium" basic sites. Large numbers of basic sites were observed from CO$_2$-TPD characterization due to the interaction between MgO and the h-BN material

Key words: ammonia synthesis; ruthenium catalyst; magnesia; hexagonal boron nitride; basicity

The synthesis of ammonia under catalytic condition has played a central role in the development of the chemical industry during the 20th century. This industrial importance has attracted significant scientific interest in understanding and improving the ammonia synthesis catalyst in recent times. Ruthenium catalysts have been investigated extensively as the second-generation catalysts for ammonia synthesis, providing remarkably higher activity at lower temperature and pressures compared with the conventional iron catalysts under similar conditions [1–4]. Over the last decade, ruthenium catalysts supported on thermally modified, partly graphitized carbon have already been applied industrially in the Kellog Brown & Root advanced ammonia process (KBRAAP) [2,3]. However, the methanation of the activated carbon support of Ru catalyst is unavoidable under the conditions of ammonia synthesis, and causes the gradual degradation of the carbon support, limiting the lifetime of Ru/C catalyst [1,3,4].

Various non-carbon supports have been investigated extensively as alternative stable supports for Ru catalyst. These include MgO [5–7], Al_2O_3 [8,9], $MgAl_2O_4$ [10], zeolites [11,12], and BN [13,14]. It has been stated that the type of support greatly influences the catalytic activity of Ru particles: the stronger the support basicity, the higher the catalytic activity [3,15–17]. Among the aforementioned supports, MgO is currently claimed to be the most suitable oxide support for Ru catalysts. In contrast to carbon, MgO is fully stable under the synthetic condition of ammonia, even at elevated temperatures. Recently, efforts have been devoted to identify excellent non-carbon support for Ru-based catalysts. Jacobsen [13] and Hansen et al. [18] have revealed that Ba promoted Ru/h-BN catalyst is the most efficient catalytic system for ammonia synthesis. Hexagonal boron nitride (h-BN) is isoelectronic with carbon, it has both crystalline and electronic structure similar to those of graphite. It also possesses excellent chemical and thermal stability, high thermal conductivity, and minimum metal-support interaction [19]. Therefore, h-BN appears to be an interesting alternative to graphite as an excellent support material for ruthenium catalyst [13,20,21]. However, h-BN is a form of covalent ceramic material, most commercial boron nitride are prepared by carbothermic reduction grounded on high temperature synthesis principles, e.g., boric acid and urea at 1000 °C [19]. Hence harsh preparative conditions are necessary for the preparation of high purity h-BN. Furthermore, h-BN is hydrophobic, which prevents ruthenium precursor and promoter depositing on its surface, thereby limiting its industrial application [19,22].

The support can influence the catalytic activity by modifying the electronic properties of the active particles and by affecting the growth and ultimately the structure and morphology of the active particles that change the abundance of the active sites of the catalyst [20]. The electronic property of MgO as well as the unique structural properties of h-BN indicates that the cooperation of MgO and h-BN, and their ability not only to increase the total basicity of catalytic system, but also to improve the efficiency of h-BN. Such modification could help to enhance the mechanical strength of h-BN and enhance the hydrophilicity of h-BN to immerse support in tetrahydrofuran (THF) solution containing $Ru_3(CO)_{12}$ in preparing Ru catalysts. Therefore, it was anticipated that it would promote the catalytic activity of the catalyst strongly. In the present work, we reported the synthesis of MgO/h-BN composite as supports for Ru catalysts and their application in the ammonia synthesis. To our knowledge, no other group has reported yet about the use of MgO/h-BN support for ruthenium catalyst for ammonia synthesis.

1 Experimental

1.1 Preparation of MgO/h-BN supports

First, 1.2 g h-BN (Alfa Aesar, AR) was mixed with 100 ml 30.8 wt% aqueous solution of $Mg(NO_3)_2$ (Sinopharm Chemical Reagent Co. Ltd, China) under stirring at ambient temperature for 1 h. Then 100 ml 9.6 wt% of aqueous solution NaOH (Sinopharm Chemical Reagent Co. Ltd, AR, China) was added gradually into the above solution containing dissolved $Mg(NO_3)_2$ under vigorous stirring to give a suspension. Thus, the precipitated $Mg(OH)_2$/h-BN was filtered and washed thoroughly with deionized water until excess of Na^+ and NO_3^- was completely removed. Finally, the filtered mass was kept in an oven to dry at 110 °C for 12 h and then calcined at 500 °C for 6 h. The obtained white powder was remarked as MgO/h-BN (mass ratio = 8:2) and simplified as MgO/h-BN[8:2]. Using the same synthetic technique other supports like MgO/h-BN[6:4], MgO/h-BN[5:5], MgO/h-BN[4:6], and MgO/h-BN[2:8] can also be prepared.

1.2 Preparation of supported Ru catalysts

Ruthenium catalysts were prepared by impregnating the

support with THF (Tianjin Chemical Reagent Co. Ltd, AR, China) solution containing $Ru_3(CO)_{12}$ (synthesized in our lab). The solution was stirred under ambient conditions for 12 h, after which the THF solvent was removed by treatment in a rotary evaporator under reduced pressure at room temperature. After drying in a vacuum at 60 °C for 12 h, the sample was reduced by flowing hydrogen (99.99%) at 300 °C for 3 h to decompose the $Ru_3(CO)_{12}$. Then Ba promoter was added to the Ru/MgO/h-BN by the impregnation method with the aqueous solution of $Ba(NO_3)_2$ (Experimental Factory of Shanghai Chemical Engineering College, AR, China) [17]. The catalysts thus, obtained had a nominal Ru content of 5.0 wt% and a calculated Ba to Ru molar ratio of 1.0. The catalysts after reduction were designated as Ba-Ru/MgO/h-BN. For comparison with pure MgO and h-BN supported ruthenium catalysts, Ba-Ru/MgO and Ba-Ru/h-BN were also prepared under the same conditions.

1.3 Measurement of catalytic activity

Catalytic reaction of ammonia synthesis were carried out in a fixed-bed stainless-steel microreactor (id = 8 mm) with a stoichiometric H_2 and N_2 mixture (H_2/N_2 = 3) flowing at temperatures ranging from 350 to 500 °C, 5.0 MPa, and 5000 h^{-1}. The purity of the H_2 or N_2 gases was over 99.99%, and the mixture was further purified before the reaction by self-designed guard containers packed with palladium catalyst and molecular sieves. The catalyst (2 ml) with particle size (20–40 mesh) was activated by a gas flow of H_2/N_2 = 3 at 450 °C for 6 h before the measurement. The ammonia synthetic activity was measured after the catalyst was stabilized at the reaction temperature at least for 2 h. The ammonia concentration at the outlet mixture was determined by a Shimadzu GC-9A with columns of Porapak QS.

1.4 Characterization of supports and ruthenium catalysts

The crystalline structure of the catalysts was analyzed by X-ray powder diffraction (XRD, X'pert, PANalytical, Dutch) using Cu K_α radiation (λ = 0.154050 nm). The chemical composition of catalyst was analyzed on an X-ray fluorescent spectrometer (PANalytical, Magix PW2403). Low-temperature nitrogen adsorption was carried out in a Micromeritics ASAP 2010 instrument at liquid nitrogen temperature to measure the surface area and pore structure of the prepared composite. The linear range of the adsorption isotherms spanning a range of p/p_0 of 0.05 to 0.35 was used to calculate the specific surface area of the samples. The Barrett-Joyner-Halenda (BJH) pore size distribution was calculated based on the desorption isotherm. The surface morphology was observed by the scanning electronic

microscopy (SEM, JSM-6701F, JEOL). High resolution transmission electron microscopy (HRTEM) experiments were conducted in a JEM-2010 TEM with an accelerating voltage of 200 kV.

H_2-TPR-MS was carried out using 10% H_2/Ar as a reducing gas in a linear quartz microreactor equipped with an MS detector (DM300, AMETEK, USA). Approximately 50 mg of a fresh catalyst was placed on top of glass wool in the reactor. The outlet of the reactor was connected to a glass column packed with molecular sieve 5A in order to remove the moisture produced from the reduction. The flow rate of the reducing gas was kept at 30 ml/min, and the temperature was raised from 25 to 650 °C at a rate of 10 °C/min. The amount of consumed H_2 was measured by a thermal conductivity detector (TCD) and calculated from the integrated peak areas of the profiles.

CO_2-TPD measurements were performed in the same apparatus. The sample (100 mg) was used and heated to 700 °C (at a heating rate of 23 °C/min) for 0.5 h in Ar atmosphere, then cooled to room temperature. Afterwards, pure CO_2 was adsorbed at room temperature for 30 min. The physisorbed CO_2 was removed by a flushing with Ar for 1 h at 120 °C. TPD was carried out in the stream of Ar at a heating rate of 20 °C/min up to 700 °C. All the samples were reduced at 450 °C for 6 h under H_2 atmosphere (99.99%) before being characterized.

2 Results and discussion

2.1 Catalytic performance for ammonia synthesis

The mass ratio of MgO to h-BN has great influence on the catalytic activity for ammonia synthesis. Figure 1 shows the catalytic activity of the Ba-promoted combination-type MgO/h-BN supported ruthenium catalysts with different ratios of MgO to h-BN under steady-state conditions. The catalytic activity of Ba-Ru/MgO catalyst for ammonia synthesis has been compared with that of Ba-Ru/MgO/h-BN catalysts under similar experimental conditions. It was obvious that the Ba-Ru/MgO/h-BN[8:2], Ba-Ru/MgO/h-BN[6:4], and Ba-Ru/MgO/h-BN[5:5] catalysts exhibited higher activity than that of conventional Ba-Ru/MgO catalyst, which was previously the most active Ru catalyst [3]. At 450 °C, the catalytic activity of Ba-Ru/MgO/h-BN[8:2], Ba-Ru/MgO/h-BN[6:4], and Ba-Ru/MgO/h-BN[5:5] catalysts were 472.5, 467.6, and 429.4 ml/(g_{cat}·h), respectively. In contrast, the conventional Ba-Ru/MgO catalyst exhibited only 272.1 ml/(g_{cat}·h) at the same experimental conditions.

2.2 XRD analysis

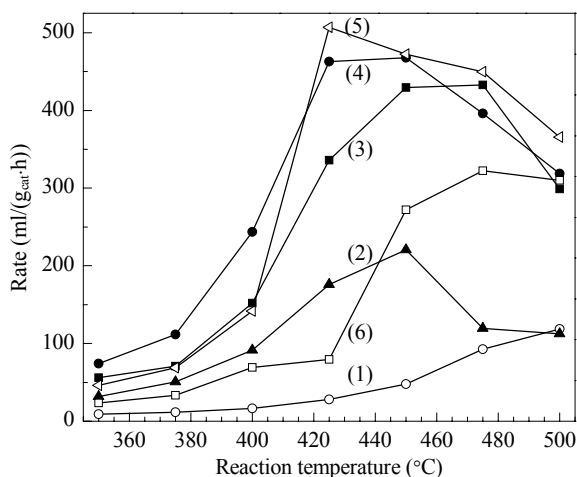The XRD patterns of MgO/h-BN composite with differ-

Fig. 1. Catalytic activity of the Ba-promoted combination-type MgO/h-BN supported ruthenium catalysts under steady-state conditions (350 − 500 °C, 5.0 MPa, and 5000 h⁻¹). (1) Ba-Ru/MgO/h-BN[2:8]; (2) Ba-Ru/MgO/h-BN[4:6]; (3) Ba-Ru/MgO/h-BN[5:5]; (4 Ba-Ru/MgO/h-BN[6:4]; (5) Ba-Ru/MgO/h-BN[8:2]; (6) Ba-Ru/MgO.

ent MgO/h-BN mass ratio are shown in Fig. 2(a). All MgO/h-BN composites showed periclase ($2\theta = 36.7°$, $42.8°$, $62.2°$, and $78.3°$, ICDD 04-0829) and h-BN phases ($2\theta = 26.7°$, $41.6°$, $50.1°$, and $55.1°$, ICDD 34-0421), respectively. The diffraction peaks of the h-BN were sharp and strong, which indicated that it was highly ordered crystal.

The XRD patterns of the reduced Ba-Ru/MgO/h-BN[8:2] catalyst and the catalyst after the activity test (used) are shown in Fig. 2(b). According to the XRD analysis, the diffraction patterns of the Ru catalysts did not provide any evidence for the presence of Ru particles despite the fact that 5 wt% Ru was loaded on the support, revealing either that the Ru particles were smaller in diameter than the detection limit of the diffractometer, or that large Ru particles (> 4 nm) were too scarce to produce detectable diffraction signals [3]. The absence of Ru peaks in the XRD characterizations could also be attributed to the Ru precursor employed. $Ru_3(CO)_{12}$ can be easily decomposed to Ru^0 metal at low temperature, avoiding the increased crystalline size because of heat treatment that result in the elimination of anionic ligands, such as chlorine [23]. Furthermore, the XRD analysis of reduced Ba-Ru/MgO/h-BN[8:2] catalyst gave signals due to $BaCO_3$ (ICDD 41-0373). It can be attributed to the reaction of BaO generation after the reduction process and CO_2 of air in the process of XRD characterization. Two consecutive steps occurred for the precursor of promoter: $Ba(NO_3)_2$ can be reduced to Ba^0 ($Ba(NO_3)_2 + 9H_2 = Ba + 2NH_3 + 6H_2O$, $\Delta G = -610.7$ kJ [2]) or to BaO ($Ba(NO_3)_2 + 8H_2 = BaO + 2NH_3 + 5H_2O$, $\Delta G = -911.4$ kJ [2]); such Ba species were amorphous, BaO would easily react with CO_2 ($BaO + CO_2 = BaCO_3$, $\Delta G = -216.7$ kJ [2])
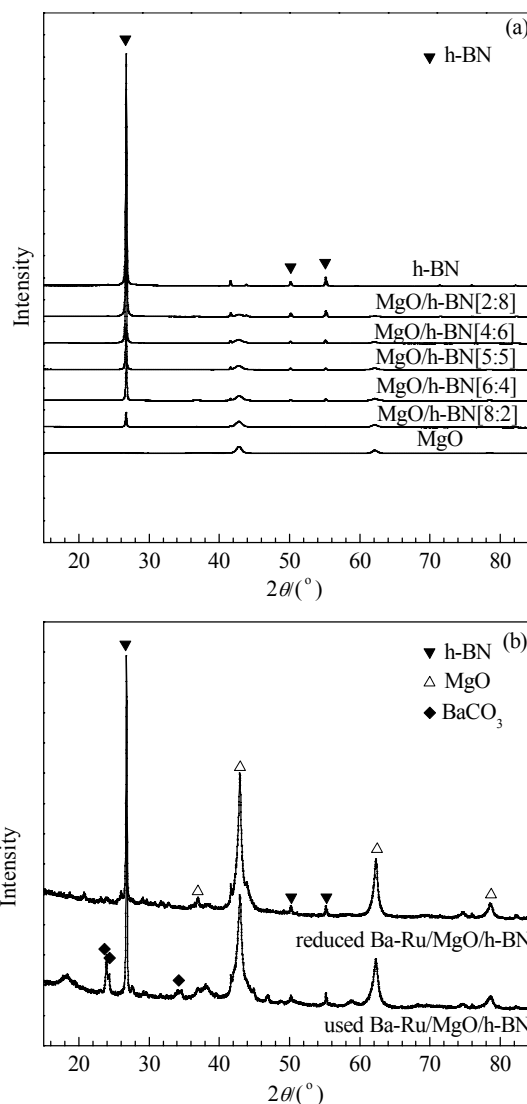

Fig. 2. XRD patterns of MgO, h-BN, and MgO/h-BN composite (a) and the reduced and used Ba-Ru/MgO/h-BN[8:2] catalyst (b).

to form the stable state of barium species in air. In contrast, $BaCO_3$ phase cannot be detected as shown in the XRD pattern of the Ba-Ru/MgO/h-BN[8:2] catalyst after the activity test. It indicated that some changes happened to Ba promoter in the ammonia synthesis. The Ba species might exist as amorphous phases after the activity tests.

2.3 Morphology of Ru particles supported on various supports

Figure 3 shows the typical morphology of Ru particles obtained from Ru/h-BN, Ba-Ru/MgO/h-BN[8:2], Ba-Ru/MgO/h-BN[6:4], and Ba-Ru/MgO/h-BN[5:5], respectively. The images were obtained after reduction by exposure to H_2 at 450 °C for 6 h. It can be observed that the Ru particles deposited on h-BN material were irregular, flat
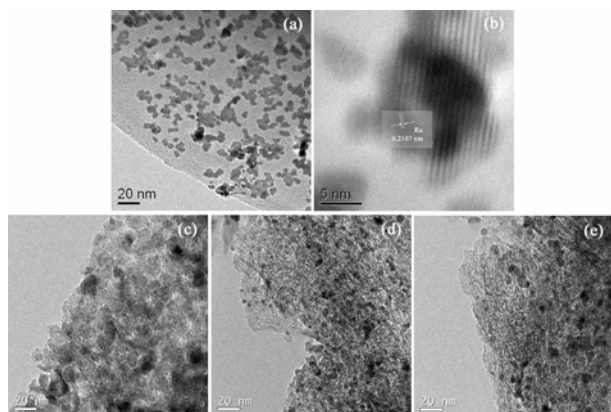
Fig. 3. TEM images of catalysts. (a, b) Ru/h-BN; (c) Ba-Ru/MgO/h-BN[8:2]; (d) Ba-Ru/MgO/h-BN[6:4]; (e) Ba-Ru/MgO/h-BN[5:5].

polygon as shown in Fig. 3(a). The HRTEM image (Fig. 3(b)) shows a lattice spacing of Ru particles of 0.2107 nm, corresponding to the (101) plane of Ru crystals [18]. Song et al. [20] confirmed the structural promotion effect of graphitized carbon by scanning tunneling microscopy, revealing that flat Ru particles were grown epitaxially on the surface of graphitized carbon hosted more B_5-sites and exhibited more surface strain than round particles. The structure of h-BN was analogous to the graphitic carbon, with strong bonding within the atomic layers and weak bonding between layers [19]. Therefore, based on our observation it was reasonable to conclude that the layered structure of h-BN could induce the epitaxial growth of flat Ru particles in a similar way to graphitized carbon as well. The MgO/h-BN composite supported Ru catalysts exhibited very different morphologies than the Ru/h-BN sample. Ruthenium particles deposited on MgO/h-BN[8:2], MgO/h-BN[6:4], and MgO/h-BN[5:5] all appeared round in shape (Figs. 3(c), 3(d), and 3(e)). It was clearly noticed that MgO/h-BN[8:2] supported Ru particles were equidimensional in size and had the smallest average size.

The morphology of the pure h-BN material and as synthesized Ba-Ru/MgO/h-BN catalysts are shown in Fig. 4. The h-BN phase existed as aggregated sheets, the sheets were arranged in stacks and appeared flaky and had an irregular shape (Fig. 4(a)). The addition of h-BN to MgO support leaded to the formation of aggregates when the mass ratio of MgO/h-BN was 5:5 as shown in Fig. 4(b), similar to Ba-Ru/MgO/h-BN[5:5], h-BN support platelets remained partially uncovered for Ba-Ru/MgO/h-BN[6:4] (Fig. 4(c)). In contrast, the MgO material was well dispersed on the h-BN surface, and the resulting coating of the h-BN support was the best of the three combination-type supported ruthenium catalysts when the MgO/h-BN weight ratio was 8:2 (Fig. 4(d)). Such observation could be related to the reactivity of the prepared catalysts (see Fig. 1) [22].
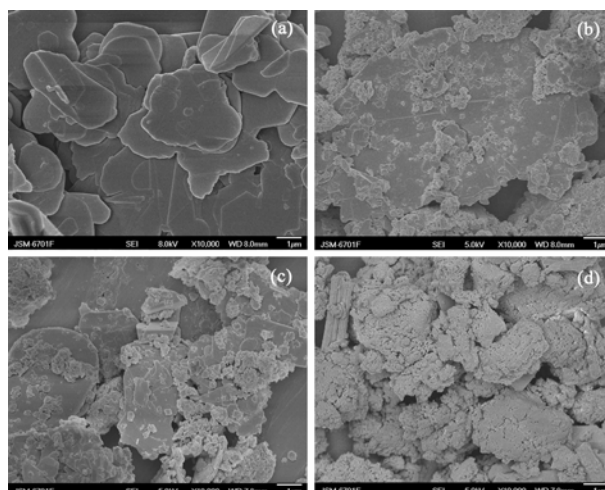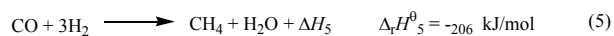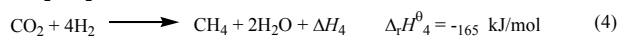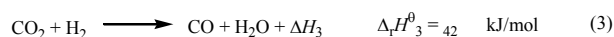

Fig. 4. SEM images of h-BN material (a), Ba-Ru/MgO/h-BN[5:5] (b), Ba-Ru/MgO/h-BN[6:4] (c), and Ba-Ru/MgO/h-BN[8:2] (d) catalysts.

2.4　H$_2$-TPR-MS analysis

The H$_2$-TPR-MS profiles of Ru/MgO and Ba-Ru/MgO/h-BN [6:4] catalysts are displayed in Fig. 5. The H$_2$ consumption during TPR measurements was ascribed to the reduction of RuO$_2$ phase because no other stable ruthenium oxide was known to exist in the solid state. Sharp signals from Ru/MgO and Ba-Ru/MgO/h-BN[6:4] catalysts were detected at the temperature (T_m) of 300–370 °C, which can be attributed to reduction of large oxide aggregates (bulk oxide). The T_m of these TPR peaks was similar to those of the temperatures reported for the complete reduction of Ru/Al$_2$O$_3$ and Ru/MgO samples (300 °C, [24,25]). However, they were higher than that of the bulk RuO$_2$ located at 217 °C [26]. Li et al. [27] proposed that this phenomenon attributed to strong interactions formed at the interface between the ruthenium species and the support. On the other hand, the low reducibility of Ru species over MgO can be also attributed to the low dispersion of Ru over low surface area support of MgO, as reported by Seetharamulu et al. [25,28].

In addition, desorption peaks attributed to $m/z = 16$, $m/z = 18$, and $m/z = 44$ were observed in the H$_2$-TPD-MS profiles. The reasons can be summarized as follows [29]:

$$MgCO_3 \longrightarrow MgO + CO_2 + \Delta H_1 \qquad \Delta_r H^\theta_1 = {}_{100\cdot6} \text{ kJ/mol} \qquad (1)$$

$$BaCO_3 \longrightarrow BaO + CO_2 + \Delta H_2 \qquad \Delta_r H^\theta_2 = {}_{271\cdot5} \text{ kJ/mol} \qquad (2)$$

$$CO_2 + H_2 \longrightarrow CO + H_2O + \Delta H_3 \qquad \Delta_r H^\theta_3 = {}_{42} \quad \text{ kJ/mol} \qquad (3)$$

$$CO_2 + 4H_2 \longrightarrow CH_4 + 2H_2O + \Delta H_4 \qquad \Delta_r H^\theta_4 = {}_{-165} \text{ kJ/mol} \qquad (4)$$

$$CO + 3H_2 \longrightarrow CH_4 + H_2O + \Delta H_5 \qquad \Delta_r H^\theta_5 = {}_{-206} \text{ kJ/mol} \qquad (5)$$

(1), (3), (4), and (5) reactions would happen on the surface of Ru/MgO catalyst, while all the reactions would happen over the surface of Ba-Ru/MgO/h-BN[6:4] catalyst.
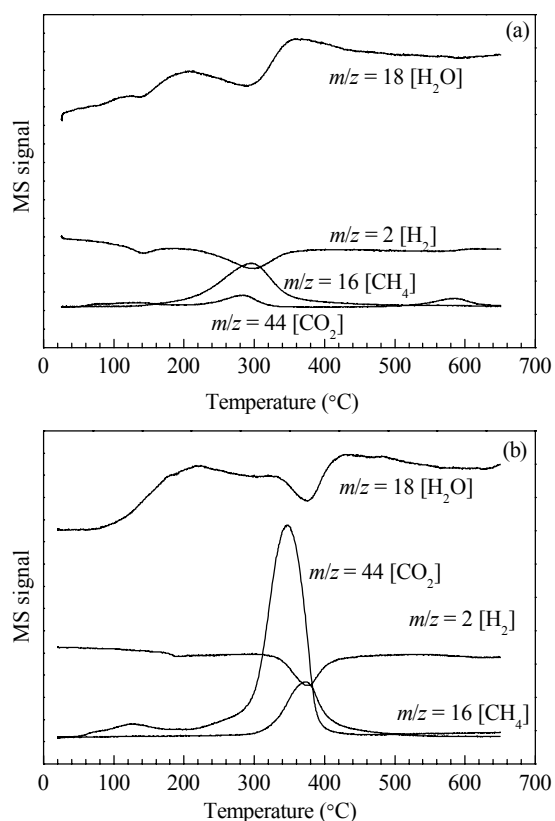
Fig. 5. H_2-TPR-MS profiles of Ru/MgO (a), Ba-Ru/MgO/h-BN[6:4] (b) catalysts.

2.5 CO$_2$-TPD analysis

The strong basicity of oxide support was known to be conductive to the activity of Ru catalysts for ammonia synthesis [3,15]. The CO$_2$-TPD method was used to measure the number and strength of the basic sites. The strength and amount of basic sites were reflected in the desorption temperature and the peak area, respectively, in a TPD profile. The surface basicity of the Ba-Ru/MgO, various Ba-Ru/MgO/h-BN and Ba-Ru/h-BN catalysts determined by the CO$_2$-TPD technique are shown in Fig. 6, and the peak area of chemisorbed CO$_2$ on these samples is listed in Table 1. The TPD profile of Ba-Ru/MgO sample contained four partially separated desorption peaks, indicating that a variety of basic sites with different strengths were presented on the surface. The basic sites of MgO was divided into three large groups exhibiting weak (CO$_2$ desorption between 27 and 147 °C), medium (CO$_2$ desorption between 147 and 377 °C), and strong (CO$_2$ desorption above 377 °C) basicity [30,31]. The weak basic sites were probably associated with Brönsted basicity and most likely with lattice-bound OH groups, while the medium and strong sites were probably associated with Lewis basicity, with the three- and four-fold-coordinated O^{2-} anions representing the strongest
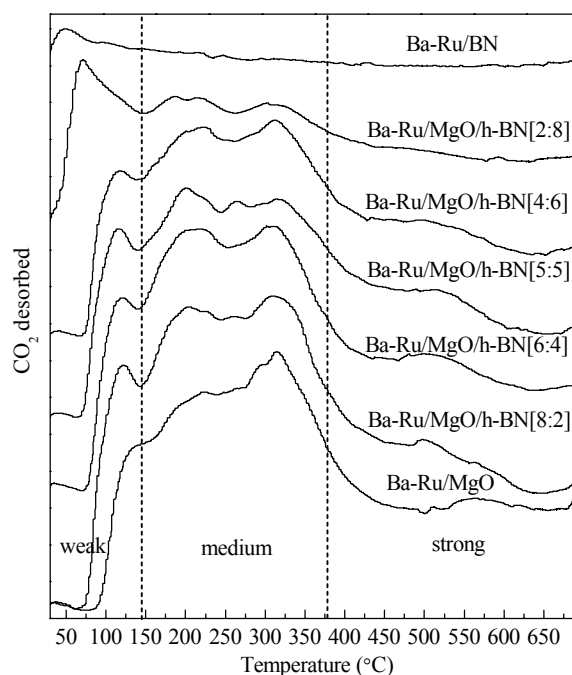

Fig. 6. CO$_2$-TPD profiles of different catalysts.

among these sites [30]. Following h-BN combination with MgO support, several changes can be observed in the TPD profiles. First, the peak corresponding to the weak basic sites which most likely were associated with hydroxyl groups was detectable from the profiles of Ba-Ru/MgO/ h-BN. Furthermore, the peak areas of all catalysts increased in the following order as listed in Table 1: Ba-Ru/h-BN < Ba-Ru/MgO/h-BN[2:8]< Ba-Ru/MgO/h-BN[4:6] < Ba-Ru/ MgO < Ba-Ru/MgO/h-BN[5:5] < Ba-Ru/MgO/h-BN[6:4] < Ba-Ru/MgO/h-BN[8:2]. Finally, in the case of Ba-Ru/h-BN catalyst there was only one small peak corresponding to weak sites, whereas the other two sites (medium and strong basic sites) completely disappeared. Activity of the Ru catalysts was explained by electron donation theory that electrons were transferred from the support or promoter to Ru metal, leading to a decreased ionization potential of Ru, thus allowing electron transfer from the metal to the anti-bonding orbits of the N atom and reducing the activation energy for the dissociative adsorption of N$_2$ molecules

Table 1 Peak area of CO$_2$-TPD measurement for Ba-Ru/MgO, various Ba-Ru/MgO/h-BN and Ba-Ru/h-BN catalysts

Catalyst	Peak area
Ba-Ru/MgO	5468.9
Ba-Ru/MgO/h-BN[8:2]	7614.8
Ba-Ru/MgO/h-BN[6:4]	6337.6
Ba-Ru/MgO/h-BN[5:5]	5498.8
Ba-Ru/MgO/h-BN[4:6]	5099.3
Ba-Ru/MgO/h-BN[2:8]	3286.5
Ba-Ru/h-BN	339.3

[15]. Aika group [3,15] proposed that the stronger the basicity of the support, the greater the catalytic activity of ruthenium catalysts for ammonia synthesis. MgO is known to be one of the most effective oxide supports, which can make ruthenium surface more electron rich and enhance the dissociation of N_2 molecules due to its electron-donating property. It can be seen clearly from the CO_2-TPD results (Fig. 6) that few weak basic sites existed over the Ba-Ru/MgO sample, while all the Ba-Ru/MgO/h-BN samples showed a sharp desorption peak assigned to weak basic sites. In addition, it was obvious that the total basic sites of Ba-Ru/MgO/h-BN[8:2], Ba-Ru/MgO/h-BN[6:4], and Ba-Ru/MgO/h-BN[5:5] were much larger than that of Ba-Ru/MgO sample as shown in Table 1. Therefore, the superior performance of Ba-Ru/MgO/h-BN[8:2], Ba-Ru/MgO/h-BN[6:4], and Ba-Ru/MgO/h-BN[5:5] catalysts can be attributed primarily to the strong basicity of combination-type of MgO/h-BN support, especially weak and medium basicity, which was conductive to enhance the electron density of Ru active sites and further increase the electron donation from its d orbital to the anti-bonding orbital of N_2, thus accelerating the dissociation of N_2 at the active site of ruthenium [8,15,17,25,28].

3 Conclusions

A series of MgO/h-BN combination-type supports were prepared by precipitating MgO on the surface of h-BN and further examined as supports for Ru catalysts for ammonia synthesis. The Ba-Ru/MgO/h-BN[8:2], Ba-Ru/MgO/h-BN[6:4], and Ba-Ru/MgO/h-BN[5:5] systems exhibited remarkable higher activity for ammonia synthesis compared with Ba-Ru/MgO, which was previously considered the most active catalyst for ammonia synthesis. The superior performance of Ba-Ru/MgO/h-BN can be attributed primarily to the large number of basic sites as well as appropriated Ru crystal size. Thus, our results indicate that MgO/h-BN composite would be an effective new type of support for ruthenium catalysts for ammonia synthesis. For the special interaction between MgO and h-BN, such combination-type composite supported ruthenium catalysts require further theoretical research.

References

1 Bielawa H, Hinrichsen O, Birkner A, Muhler M. *Angew Chem, Int Ed*, 2001, **40**: 1061

2 Truszkiewiz E, Raróg-Pilecka W, Schmidt-Szałowski K, Jodzis S, Wilczkowska E, Łomot D, Kaszkur Z, Karpiński Z, Kowalczyk Z. *J Catal*, 2009, **265**: 181

3 You Z, Inazu K, Aika K, Baba T. *J Catal*, 2007, **251**: 321

4 Liang C H, Li Z L, Qiu J S, Li C. *J Catal*, 2002, **211**: 278

5 Xu Q C, Lin J D, Fu X Z, Liao D W. *Catal Commun*, 2008, **9**: 1214

6 Iwamoto J, Itoh M, Kajita Y, Saito M, Machida K. *Catal Commun*, 2007, **8**: 941

7 Wu S, Chen J X, Zheng X F, Zeng H S, Zheng C M, Guan N J. *Chem Commun*, 2003: 2488

8 Murata S, Aika K. *J Catal*, 1992, **136**: 110

9 Miyazaki A, Balint I, Aika K, Nakano Y. *J Catal*, 2001, **204**: 364

10 Jacobsen C J H, Dahl S, Hansen P L, Törnqvist E, Jensen L, Topsøe H, Prip D V, Møenshaug P B, Chorkendorff I. *J Mol Catal A*, 2000, **163**: 19

11 McClaine B C, Becue T, Lock C, Davis R. *J Mol Catal A*, 2000, **163**: 105

12 Cisneros M D, Lunsford J H. *J Catal*, 1993, **141**: 191

13 Jacobsen C J H. *J Catal*, 2001, **200**: 1

14 Szmigiel D, Raróg-Pilecka W, Miśkiewicz E, Maciejewska E, Kaszkur Z, Sobczak J W, Kowalczyk Z. *Catal Lett*, 2005, **100**: 79

15 Aika K, Ohya A, Ozaki A, Inoue Y, Yasumori I. *J Catal*, 1985, **92**: 305

16 Larichev Y V, Moroz B L, Zaikovskii V I, Yunnusov S M, Kalyuzhnaya E S, Shur V B, Bukhtiyarov V I. *J Phys Chem C*, 2007, **111**: 9427

17 Aika K, Taknao T, Murata S. *J Catal*, 1992, **136**: 126

18 Hansen T W, Wagner J B, Hansen P L, Dahl S, Topsøe H, Jacobsen C J H. *Science*, 2001, **294**: 1508

19 Paine R T, Narula C K. *Chem Rev*, 1990, **90**: 73

20 Song Z, Cai T H, Hanson J C, Rodriguez J A, Hrbek J. *J Am Chem Soc*, 2004, **126**: 8576

21 Jacobsen C J H. US 6 479 027. 2002

22 Postole G, Gervasine A, Caldararu M, Bonnetot B, Auroux A. *Appl Catal A*, 2007, **325**: 227

23 Moggi P, Predieri G, Albanesi G, Papadopulos S, Sappa E. *Appl Catal*, 1989, **53**: L1

24 Yang X L, Zhang W Q, Xia C G, Xiong X M, Mu X Y, Hu B. *Catal Commun*, 2010, **11**: 867

25 Seetharamulu P, Kumar V S, Padmasri A H, Raju B D, Rama Rao K S. *J Mol Catal A*, 2007, **263**: 253

26 Siva Sankar Reddy P, Pasha N, Chalapathi Rao M G V, Lingaiah N, Suryanarayana I, Sai Prasad P S. *Catal Commun*, 2007, **8**: 1406

27 Li D, Ichikuni N, Shimazu S, Uematsu T. *Appl Catal A*, 1999, **180**: 227

28 Seetharamulu P, Hari Prasad Reddy K, Padmasri A H, Rama Rao K S, Raju B D. *Catal Today*, 2009, **141**: 94

29 霍超, 夏庆华, 骆雁, 杨霞珍, 刘化章. 催化学报 (Huo Ch, Xia Q H, Luo Y, Yang X Zh, Liu H Zh. *Chin J Catal*), 2009, **30**: 537

30 Liu Z, Cortés-Concepción J A, Mustian M, Amiridis M D. *Appl Catal A*, 2006, **302**: 232

31 Kuś S, Otremba M, Tórz A, Taniewski M. *Appl Catal A*, 2002, **230**: 263